Available online at www.sciencedirect.com
ScienceDirect
Journal of Power Sources 159 (2006) 721–727
JOURNAL OF POWER SOURCES
www.elsevier.com/locate/jpowsour

Kinetics of precipitation hardening in Pb–0.08 wt.%Ca–*x* wt.%Sn alloys by in situ resistivity measurements

M. Dehmas [a,*], A. Maître [b], J.B. Richir [b], P. Archambault [a]

[a] *LSG2M, UMR CNRS 7584, Ecole des Mines, Parc de Saurupt, F-54042 Nancy Cedex, France*
[b] *LCSM, UMR CNRS 7555, Université Henri Poincaré, Nancy I, BP 239, F-54506 Vandoeuvre-les-Nancy Cedex, France*

Received 7 April 2005; accepted 28 July 2005
Available online 6 January 2006

Abstract

The effects of tin content and annealing temperature on the transformation sequences of Pb–0.08 wt.%Ca–*x* wt.%Sn supersaturated alloys (with $x = 0.6$, 1.2 and 2.0%) have been firstly studied from TEM observations and hardness measurements. Secondly, the age-hardening kinetics of these ternary alloys during isothermal holdings have been characterized by electrical resistivity measurements. In particular, it appeared that increase of tin content both delayed the main metallurgical stages and is accompanied by suppression of the first discontinuous reactions of ageing when the Sn/Ca ratio value is above 9. Moreover, the ageing kinetics are accelerated when increasing the annealing temperature because of the solute diffusion activation.

Keywords: Lead alloys; Ageing; Overageing; Kinetics; Electrical resistivity; Hardness

1. Introduction

Pb–Ca–Sn alloys have been extensively used as positive electrode substrate of maintenance-free lead acid battery in applications such as the starting–lighting–ignition of vehicles, standby powder or storage in photovoltaic systems [1]. The electrochemical behaviour of Pb–Ca–Sn alloy grids in particular in the most severe conditions, i.e. in overcharge conditions, depends on their metallurgical state [2,3].

Ageing of Pb–0.08 wt.%Ca–*x* wt.%Sn alloys at room temperature is usually characterized by several steps [4]: two preliminary discontinuous transformations (more or less complete), followed by a continuous precipitation of the $L1_2$ hardening phase which composition obeys to the $(Pb_{(1-x)}Sn_x)_3Ca$ solid solution [5]. When the weight ratio Sn/Ca (r) is higher than 9, the continuous precipitation occurs preferentially [5]. The overageing that is accompanied by a Pb–Ca–Sn alloy softening can be described through two successive steps [6]: the re-precipitation of coarse $L1_2$ precipitates and the lamellar coalescence of these latter precipitates.

Even if recent works allowed a better understanding of the sequence of transformations during the ageing or overageing, few kinetic studies of age-hardening exists for the Pb–Ca–Sn alloys near room temperature (i.e. for the working conditions of lead acid battery). Only, a very recent study [7] consisted in the definition of the adequate annealing treatment for the Pb–0.08 wt.%Ca–2.0 wt.%Sn composition from Small Angle Neutron Scattering (S.A.N.S.) and resistivity measurements.

Consequently, the aim of the present paper is to determine the kinetics of precipitation hardening for the as cast Pb–0.0.8 wt.%Ca–*x* wt.%Sn alloy as a function of tin content and annealing temperature by in situ resistivity measurements. Also, these results as well as hardness measurements and microstructural observations performed during the present study allow to determine the role played by tin content on the age-hardening process.

2. Experimental procedure

2.1. Synthesis of Pb–Ca–Sn alloys

Pb–0.08 wt.%Ca–*x* wt.%Sn alloys ($x = 0.6$, 1.2 and 2) were synthesized through melting of stoichiometric mix-

* Corresponding author. Tel.: +33 5 6288 5653; fax: +33 3 6288 5663.
E-mail address: Moukrane.Dehmas@ensiacet.fr (M. Dehmas).

0378-7753/$ – see front matter © 2005 Elsevier B.V. All rights reserved.
doi:10.1016/j.jpowsour.2005.07.094

Table 1
Chemical analysis of alloys measured by electron microprobe

Alloy	Pb (wt.%)	Ca (wt.%)	Sn (wt.%)
Pb–0.08%Ca–0.6%Sn	99.34	0.070	0.583
Pb–0.08%Ca–1.2%Sn	98.85	0.060	1.082
Pb–0.08%Ca–2%Sn	98.00	0.065	1.930

tures of master alloys and the pure elements. The lower alloy tin content (i.e. 0.6 wt.%) was synthesized from the Pb–0.112%Ca–0.245%Sn master alloy (provided by Compagnie Européenne d'Accumulateurs), pure lead (99.999%, Goodfellow) and pure tin (99.999% from Cerac). The alloys with 1.2 and 2% Sn were elaborated from the Pb–0.08%Ca–1.05%Sn master alloy and pure tin. The mixture was melted at 650 °C during one hour under flowing argon in order to ensure compositional homogeneity then cast in an iced aluminium mould (60 mm × 60 mm × 3 mm). Then, the ingots were divided by cutting the initial plates into rods (Ø = 3 mm, L = 35 mm) for further characterizations and kept in liquid nitrogen between each measurement to inhibit the phase transformations. The composition of these ternary alloys is reported in Table 1.

2.2. In situ electrical resistivity measurement

The in situ electrical resistivity measurement is based on the four points method: a constant current of 2 A is sent through the sample with pure platinum wires [8]. The resulting potential difference between the two inner points is amplified ($\times 10^4$) and acquired by the computer. The whole device was introduced in a thermostated silicon oil bath cell in order to perform the heat treatment. The temperature was real time controlled with a K thermocouple welded on the sample and a platinum probe plunged in the bath. Considering that the electrical resistivity of the alloy depends mainly on temperature and concentrations of elements in solid solution, and in order to increase the sensitivity of the measurement, the electrical resistivity of pure lead (versus temperature) was subtracted from the experimental signal of the sample at each temperature.

2.3. Microstructure characterization

The characterization of the Pb–Ca–Sn alloy microstructure was performed using transmission electron microscopy (Philips-CM20 operating at 200 kV) and optical microscopy (Olympus Vanox AHMT). Thin foils for TEM observations were prepared by coupling microtomy (Ultramicrotome Reichert Ultracute) and argon ion-beam thinning (Gatan Model 691 apparatus) as described elsewhere [9]. For optical examinations, the microstructures were revealed in two steps that may be summarized as follows:

(i) specimens were immersed five times for 30 seconds in a solution of acetic acid (80 vol.%) and H_2O_2 (20 vol.%); between two immersions, the samples were rinsed in a concentrated acid acetic solution;

(ii) then, the specimens were plunged for 10 seconds in a aqueous solution composed of citric acid (25 vol.%) and ammonium molybdate (10 vol.%).

2.4. Hardness measurement

The evolution of mechanical properties associated with the phase transformations was followed by Vickers hardness measurements performed under 1 kgf load using a Wolpert Dia-Testor II hardness tester. Isothermal experiments were carried out at room temperature, 80 and 120 °C. The hardness data reported were determined from at least five readings for each sample.

3. Experimental results and discussion

3.1. Hardness measurements

As mentioned in literature [4], for the lower (Sn/Ca) weight ratio ($r < 9$) (e.g. Pb–0.08%Ca–0.6%Sn alloy), the corresponding hardness curve during isothermal holding exhibits three steps (Fig. 1). The first step (called A) can be associated to the first discontinuous transformation. The second discontinuous transformation (B effect) namely called "puzzling" leads to a hardness around 15 HV. At last, the $L1_2$ phase continuous microprecipitation (C effect) leads to the peak hardness, i.e. 20 HV.

After two hours at 120 °C, softening appears and, consequently, indicates the overageing appearance.

When increasing the Sn/Ca weight ratio ($r > 9$), one can notice in Fig. 2 the suppression of the two first steps (the hardness monotonously rises from pure lead hardness (5 HV) up to the peak hardness). Moreover, the peak hardness increases when rising the tin content: at 120 °C, 20 to 30 HV for the Pb–0.08%Ca–0.6%Sn and Pb–0.08%Ca–2.0%Sn alloys, respectively.

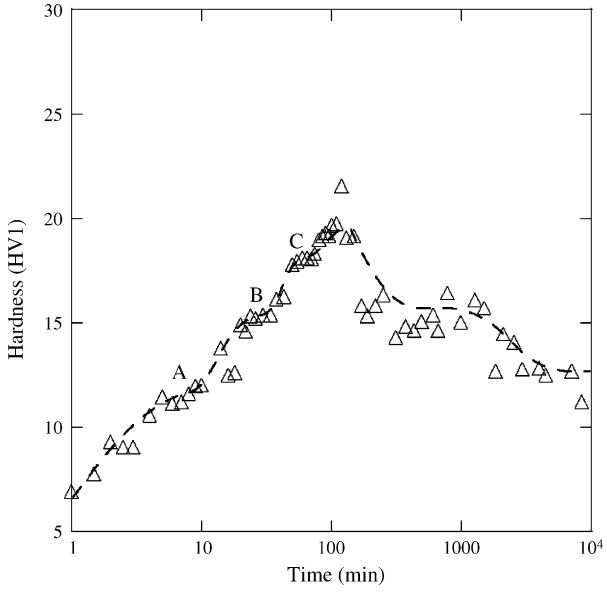

Fig. 1. Hardness evolution at 120 °C for the as cast Pb–0.08%Ca–0.6%Sn alloy.

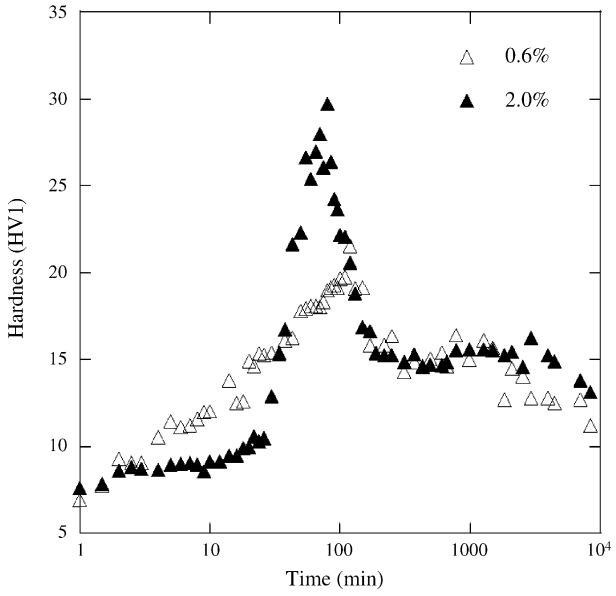

Fig. 2. Hardness evolution at 120 °C for the as cast Pb–0.08%Ca–0.6%Sn and Pb–0.08%Ca–2.0%Sn alloys.

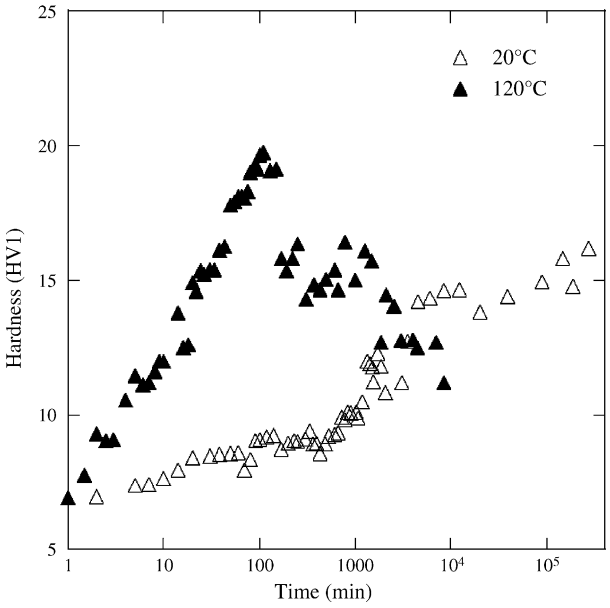

Fig. 3. Hardness evolution at room temperature and at 120 °C for the as cast Pb–0.08%Ca–0.6%Sn alloy.

The disappearance of the preliminary reactions could be associated to the tin segregation that must be effective for alloy tin content equal or superior to 1 wt.%. Indeed, this value corresponds to the tin content of PbSn alloy when the thermodynamic equilibrium is reached [10]. In these conditions, the tin segregation could inhibit the movement of the discontinuous transformation fronts [11]. Therefore, the rise of the hardness maximum could be correlated to the increase of the $L1_2$ volume fraction: indeed, the Pb–Ca–Sn phase diagram [4,12] suggests a decrease of the calcium solid solubility in (α-Pb) when tin is added.

Comparison of hardness curves obtained at several temperatures (Fig. 3) clearly shows an acceleration of the hardening and softening effects when increasing the annealing temperature. For the higher alloy tin content, the incubation time is divided by six between room temperature and 120 °C. This result must be attributed to the activation of element diffusion at the higher temperatures.

3.2. Microstructural observations

Fig. 4a shows the microstructure of the as cast Pb–0.08%Ca–0.6%Sn alloy which is characterized by a dendritic sub-structure resulting from the tin and calcium segregation. In particular, this segregation effect can be observed for the higher cooling rates of samples, i.e. equal or superior to 40 °C s^{-1}.

The microstructure of Pb–0.08%Ca–0.6%Sn alloy undergoes progressive changes with annealing time at 120 °C. The early discontinuous stages of ageing are characterized by two steps as a function of annealing time:

(i) a rapid step that is characterized by an irregular and incomplete displacement of (sub-)grain boundary [4]. From literature, the driving force of this stage is attributed to a disorder–order transformation for the (α-Pb) lead solid solution [13]. This discontinuous transformation leads to the formation of "puzzled" grains (Fig. 4b).

(ii) A second stage which takes place for longer times is characterized by a fine precipitation of the $L1_2$ $(Pb_{1-x}Sn_x)_3Ca$ phase (Fig. 5).

The microstructures shown in Fig. 4b and Fig. 4c indicate that the grain shape varies with the Ca/Sn weight ratio. So, for the higher values ($r > 9$), the grain shape becomes more regular by suppression of the preliminary discontinuous transformations. On this specific point, previous studies [14] suggested that when the Sn/Ca weight ratio exceeds 9 the grains are well defined and larger in size. This effect can be explained from the lower calcium solubility when increasing the tin content. Indeed, the excess of calcium forms precipitates and a fine grain structure is expected.

3.3. In situ electrical resistivity

3.3.1. Effect of the annealing temperature

The evolution of the differential electrical resistivity for the as cast Pb–0.08 wt.%Ca–2 wt.%Sn alloy on heating at 6 °C min^{-1} is shown in Fig. 6. The values of electrical resistivity are in the range 0.9–2.15 μΩ cm. One can observe a linear variation between room temperature and around 90 °C followed by a more significant decrease up to 125 °C and a slowing down at higher temperature.

This behaviour seems to indicate that the $L1_2$ phase precipitation occurs successively in two different steps when increasing the temperature.

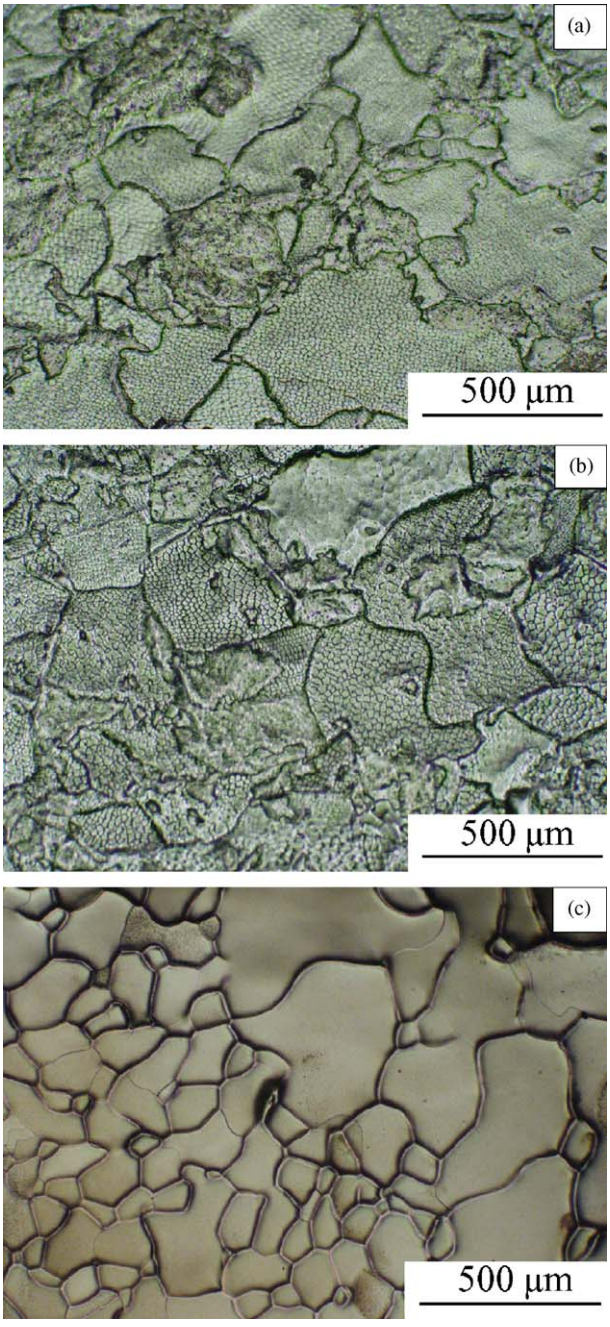

Fig. 4. Microstructures of the as cast Pb–0.08%Ca–0.6%Sn alloy (a), of the Pb–0.08%Ca–0.6%Sn alloy annealed 30 min at 120 °C (b) and of the Pb–0.08%Ca–2.0%Sn alloy annealed 30 min at 120 °C (c).

It can be noticed that this behaviour is also observed for the two other alloys with different tin contents (i.e. 0.6 and 1.2 wt.%). The electric resistivity values and inflexion temperatures are only modified.

In order to study the transformation kinetics during isothermal holdings, the samples were heated at about 20 °C s^{-1} up to the holding temperature as no phase transformation was detected for such a heating rate whatever the tin content. The holding temperatures have been chosen equal to 40, 80 and 120 °C with respect to the working temperature of the acid battery or the

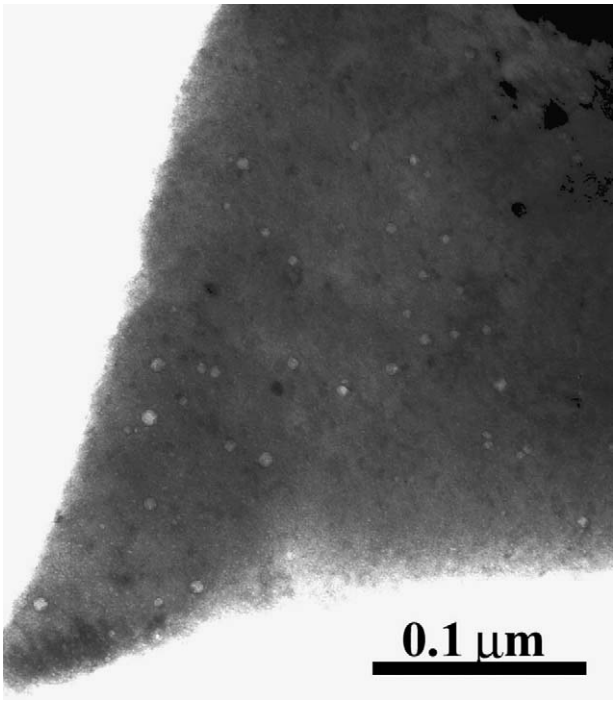

Fig. 5. TEM bright field image (zone axis [1 1 0]) of Pb–0.08%Ca–0.6% alloy annealed 1 h at 120 °C.

synthesis conditions of the active matter for the battery industry [2]. The evolution of the electrical resistivity recorded for Pb–0.08%Ca–2%Sn alloy during isothermal holdings are presented in Fig. 7a.

Whatever the holding temperature, the resistivity decreases immediately: no incubation time is detected, suggesting that the $L1_2$ phase precipitation starts very fast due to the high supersaturation. After a long time, an equilibrium is reached with a resistivity level strongly depending on the holding temperature.

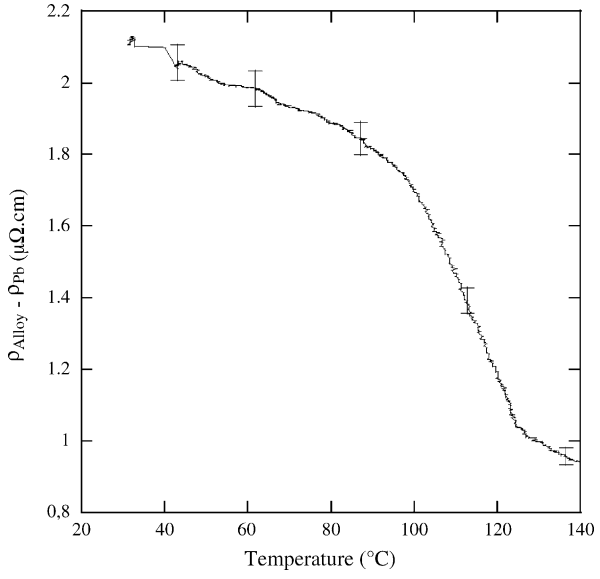

Fig. 6. Evolution of the resistivity for the as cast Pb–0.08%Ca–2%Sn alloy during heating at 6 °C min^{-1}.

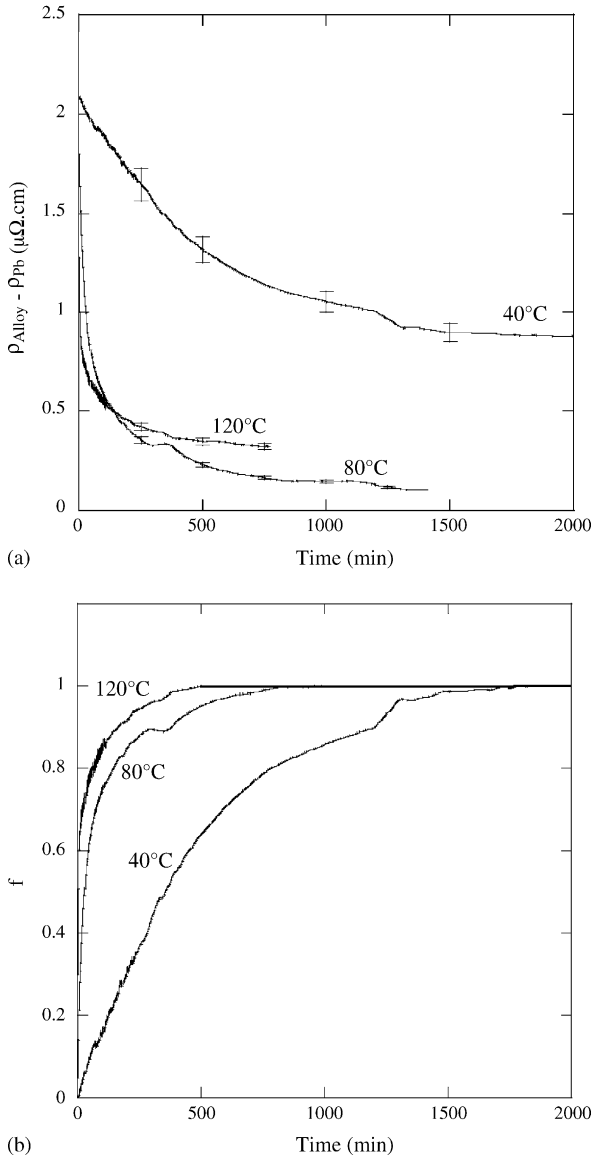

Fig. 7. Isothermal electrical resistivity variations (a) and associated normalized kinetics (b) for the Pb–0.08%Ca–2%Sn alloy. Continuous heating at about 20 °C s^{-1} (from as cast state) interrupted by isothermal holding at different temperatures.

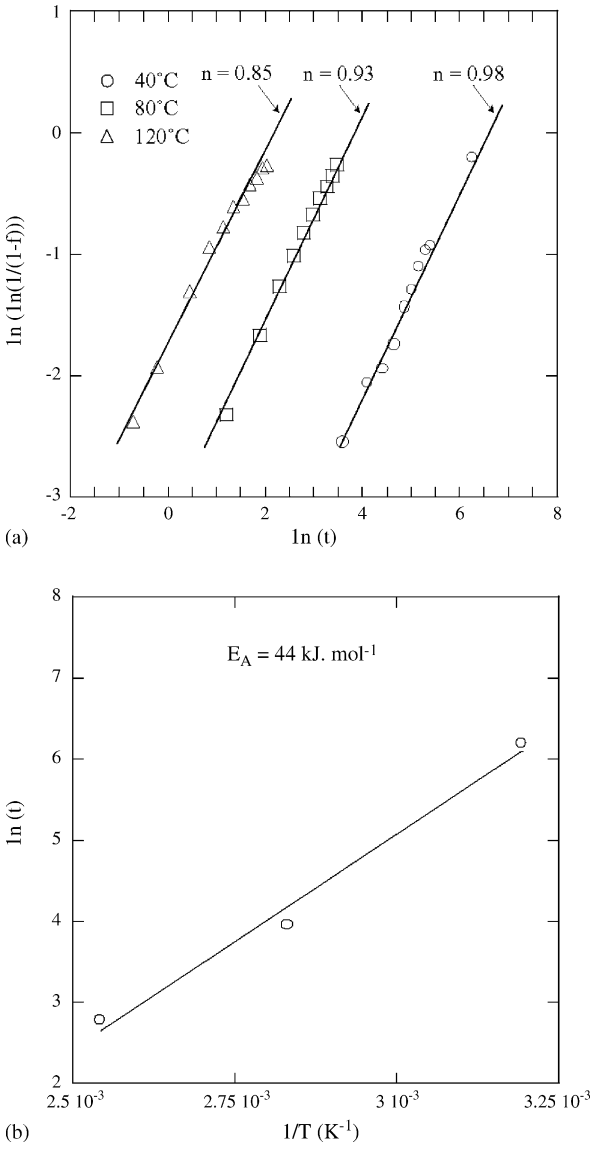

Fig. 8. Typical plots of $\ln(\ln(1-f))$ vs. ageing time at several temperatures (a) and the corresponding Arrhenius representation (b) in Pb–0.08%Ca–2.0.%Sn alloy.

From resistivity measurements, the fraction f of the reaction of $L1_2$ precipitation is taken to:

$$f = \frac{\rho_0 - \rho_t}{\rho_0 - \rho_\infty} \quad (1)$$

where ρ_0 is the initial resistivity at considered temperature, ρ_t the resistivity at considered holding time and ρ_∞ is the resistivity at the equilibrium state. So, the fraction of $L1_2$ precipitation is reported in Fig. 7b at three temperatures: 40, 80 and 120 °C. From these results, it appears that that the precipitation kinetics are accelerated when increasing the holding temperature.

Therefore, the time dependence of the fraction of precipitation occurred at constant temperature will be expressed by Johnson-Mehl-Avrami law:

$$f = 1 - \exp(-Kt^n) \quad (2)$$

where f is the transformed fraction, t the ageing time, n and K constant. The K coefficient obeys to the Arrhenius law as a function of the temperature:

$$K = A \exp\left(-\frac{E_A}{RT}\right) \quad (3)$$

where A is constant and E_A the activation energy. The determination of activation energy depends on the measurement of time corresponding to the fixed value of transformed fraction ($f = 1 - \exp(-1) = 0.632$).

The n values and the activation energy are determined from Fig. 8a and Fig. 8b, i.e. from $\ln(\ln(1/(1-f)))$ versus $f(\ln t)$ and $\ln t$ versus $f(1/T)$ representations, respectively. For Pb–0.08%Ca–2.0%Sn alloy, the n values so obtained tend to one with decreasing the temperature (see Fig. 8a). This n value could be associated to a discontinuous transformation mecha-

nism in two steps: a rapid nucleation and a rate-limiting growth stage which is accompanied by the grain boundary diffusion of Pb, Ca and Sn species [15]. Nevertheless, this hypothesis seems to be in accordance with the experimental results obtained at the lower temperature when the discontinuous process is sufficiently slow. But, when rising temperature, only the continuous precipitation occurs and, consequently, the n value diverges from 1.

Otherwise, the activation energy that is calculated from Arrhenius representation (see Fig. 8b), i.e. 44 kJ mol^{-1}, is coherent with those reported in the literature for the continuous precipitation [4,6]. This energy is lower that the lead-diffusion enthalpy (104 kJ mol^{-1}) because the lead diffusion proceeds on short-circuits such as grain boundaries or dendritic (sub-)boundaries. So, the present value is equal to this determined for the lead diffusion on grain boundaries [16].

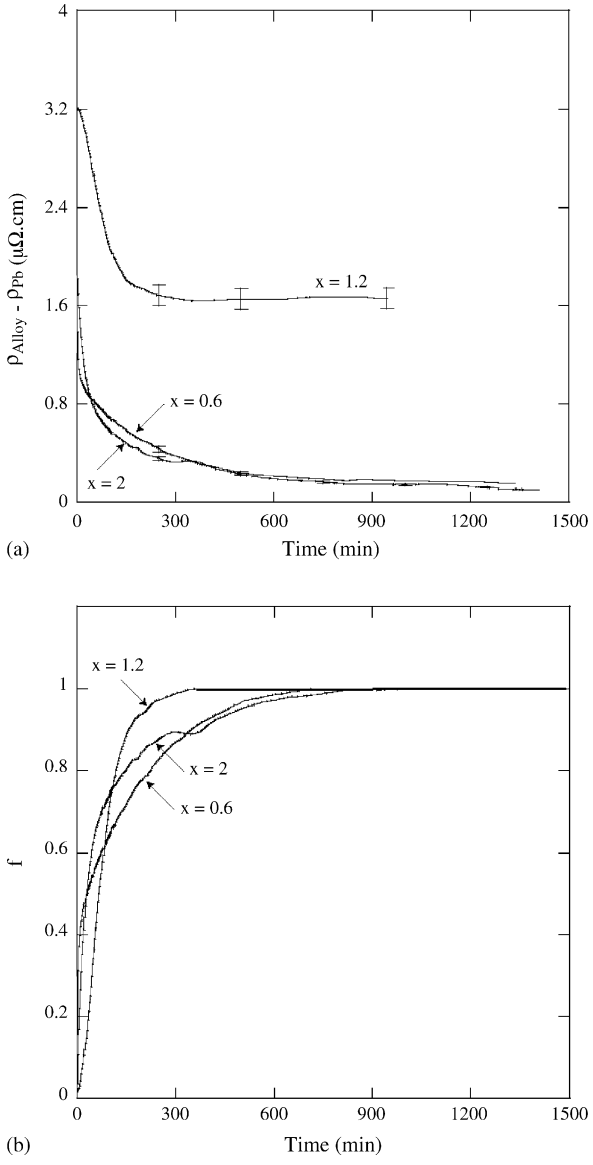

Fig. 9. Isothermal electrical resistivity variations (a) and associated normalized kinetics (b) for Pb–0.08%Ca–x%Sn alloys. Continuous heating at about 20 °C s^{-1} (from as cast state) interrupted by isothermal holding at 80 °C.

3.3.2. Effect of the alloy tin content

A similar approach can be used to precise the effect of tin content on the precipitation kinetics. For an isothermal holding at 80 °C and different tin contents of Pb–0.08%Ca–x%Sn alloy (x = 0.6, 1.2 and 2), the corresponding resistivity evolutions and normalized curves are reported in Fig. 9a and Fig. 9b, respectively. When rising the tin content, the $L1_2$ phase precipitation kinetic appears to be delayed which is not really surprising since the supersaturation effect is more significant when increasing the alloy tin content [9], leading to a higher time to reach the equilibrium. For the Pb–0.08%Ca–1.2%Sn alloy, the equilibrium is reached very quickly because this alloy contains less calcium than the two others (see Table 1).

4. Conclusion and outlooks

In this paper, the effects of the tin content and temperature on the transformation sequences and on the age-hardening kinetics of Pb–0.08%Ca–x%Sn alloys have been discussed. For the age-hardening stage, the sequence of transformations seems to be sensitive to the initial weight Sn/Ca ratio as mentioned in literature [4]. In particular, the suppression of the preliminary reactions is observed when the ratio value is above 9.

It has been shown that the ageing kinetics are accelerated when increasing the annealing temperature because of the solute diffusion improvement. Conversely, tin additions would delay the ageing or overageing appearance by rising the initial supersaturation degree of ternary alloys.

Further works will allow to establish the temperature–time-transformation diagrams for these alloys by characterizing the evolution of the microstructure during the isothermal holdings in order to associate the contribution of each hardening step with the electrical resistivity evolution. Such diagrams would allow to define some adequate annealing treatments which would stop the overageing for the Pb–0.08%Ca–x%Sn alloys and consequently, would maintain their mechanical properties and their electrochemical resistance in sulphuric acid at higher and steady levels.

At last, these annealing treatments will be coherent with the acid battery manufacturing and, in particular, with the steps of curing, drying and formation of the active matter.

Acknowledgement

The authors are grateful to Mr. Y. Ravaux of the Microscopy and Microanalysis Service of University of Nancy (France) for technical help in particular for EPMA analyses.

References

[1] J. Perkins, G.R. Edwards, J. Mater. Sci. 10 (1975) 136–158.
[2] E. Jullian, L. Albert, J.L. Caillerie, J. Power Sources 116 (2003) 185–192.
[3] G. Bourguignon, A. Maître, E. Rocca, J. Steinmetz, L. Torcheux, J. Power Sources 113 (2003) 301–307.
[4] L. Bouirden, J.P. Hilger, J. Hertz, J. Power Sources 33 (1991) 27–50.
[5] J. Hertz, C. Fornasieri, J.P. Hilger, M. Notin, J. Power Sources 46 (1993) 299–310.

[6] A. Maître, G. Bourguignon, J.M. Fiorani, J. Steinmetz, J. Ghanbaja, Mater. Sci. Eng. A 340 (2003) 103–113.
[7] A. Maître, G. Bourguignon, G. Medjahdi, E. McRae, M.H. Mathon, Scripta Mater. 50 (2004) 685–689.
[8] M. Dehmas, P. Archambault, M. Serriere, E. Gautier, Ch.A. Gandin, Aluminium 78 (2002) 864–869.
[9] A. Maître, G. Bourguignon, J.M. Fiorani, J. Ghanbaja, J. Steinmetz, Mater. Sci. Eng. A 358 (2003) 233–242.
[10] I. Karkaya, W.T. Thompson, Bull. Alloys Phase Diagram 9 (1987) 144.
[11] H. Tsubakino, N. Tagami, S. Ioku, A. Yamamoto, Metall. Mater. Trans. A 27 (1996) 1675–1682.
[12] Y. Cartigny, J.M. Fiorani, A. Maître, M. Vilasi, Intermetallics 11 (2003) 1205–1210.
[13] J.P. Hilger, A. Boulahrouf, Mater. Charact. 24 (2) (1990) 159–167.
[14] C.S. Lakshmi, J.E. Manders, D.M. Rice, J. Power Sources 73 (1998) 23–29.
[15] J.W. Christian, The Theory of Transformation in Metals and Alloys, vol. 1, third ed., Pergamon Edition, Oxford, 2002.
[16] D. Gupta, K. Vieregge, W. Gust, Acta Mater. 47 (1998) 5–12.